International Journal of Pharmaceutics 533 (2017) 225–235

Contents lists available at ScienceDirect

International Journal of Pharmaceutics

journal homepage: www.elsevier.com/locate/ijpharm

Research paper

Experimental and computational study of the effect of breath-actuated mechanism built in the NEXThaler® dry powder inhaler

Árpád Farkas[a,*], David Lewis[b], Tanya Church[b], Alan Tweedie[b], Francesca Mason[b], Allen E. Haddrell[c], Jonathan P. Reid[c], Alpár Horváth[d], Imre Balásházy[a]

[a] Centre for Energy Research, Hungarian Academy of Sciences, Konkoly-Thege Miklós út 29-33, 1121, Budapest, Hungary
[b] Chippenham Research Centre, Chiesi Limited, Chippenham, Wiltshire, SN14 0AB, UK
[c] School of Chemistry, University of Bristol, Bristol, BS8 1TS, UK
[d] Chiesi Hungary Ltd., Dunavirág u. 2, 1138, Budapest, Hungary

ARTICLE INFO

Keywords:
Breath-actuated mechanism
Aerosol drug targeting
Beclomethasone dipropionate
Formoterol fumarate
Particle size distribution
Airway deposition modelling
Hygroscopic growth

ABSTRACT

The breath-actuated mechanism (BAM) is a mechanical unit included in NEXThaler® with the role of delaying the emission of the drug until the inhalation flow rate of the patient is sufficiently high to detach the drug particles from their carriers.

The main objective of this work was to analyse the effect of the presence of BAM on the size distribution of the emitted drug and its airway deposition efficiency and distribution. Study of the hygroscopic growth of the emitted drug particles and its effect on the deposition was another goal of this study.

Size distributions of Foster® NEXThaler® drug particles emitted by dry powder inhalers with and without BAM have been measured by a Next Generation Impactor. Three characteristic inhalation profiles of asthmatic patients (low, moderate and high flow rates) were used for both experimental and modelling purposes. Particle hygroscopic growth was determined by a new method, where experimental measurements are combined with simulations. Upper airway and lung deposition fractions were computed assuming 5 s and 10 s breath-hold times.

By the inclusion of BAM the fine particle fraction of the steroid component increased from 24 to 30% to 47–51%, while that of bronchodilator from 25–34% to 52–55%. The predicted upper airway steroid and bronchodilator doses decreased from about 60% to 35–40% due to BAM. At the same time, predicted lung doses increased from about 20%–35% (steroid) and from 22% to 38% (bronchodilator) for the moderate flow profile and from about 25% to 40% (steroid) and from 29% to 47% (bronchodilator) for the high inhalation flow profile. Although BDP and FF upper airway doses decreased by a factor of about two when BAM was present, lung doses of both components were about the same in the BAM and no-BAM configurations at the weakest flow profile. However, lung dose increased by 2–3% even for this profile when hygroscopic growth was taken into account.

In conclusion, the NEXThaler® BAM mechanism is a unique feature enabling high emitted fine particle fraction and enhanced drug delivery to the lungs.

1. Introduction

Foster® NEXThaler® is an ICS + LABA (inhaled corticosteroid and long-acting β2-agonist) fixed combination aerosol drug used in current COPD and asthma therapy (Crisafulli et al., 2016). According to the SPC (summary of product characteristics) of Foster® NEXThaler® each metered dose of 10 mg powder contains 100 micrograms of beclometasone dipropionate anhydrous (BDP) and 6 micrograms of formoterol fumarate dihydrate (FF). As excipients, Foster® NEXThaler® contains lactose monohydrate (about 9.9 mg, which contains small amounts of milk protein), and magnesium stearate.

Based on the experimental measurements of several investigators

Abbreviations: ACI, Andersen Cascade Impactor; ACN, acetonitrile; BAM, breath-actuated mechanism; BDP, beclomethasone dipropionate; BH, breath-hold time; CK-EDB, comparative kinetic electrodynamic balance; DD, delivered dose; DPI, dry powder inhaler; DUSA, dosing unit sampling apparatus; EPF, extrafine particle fraction; FF, formoterol fumarate; FPF, fine particle fraction; GF, growth factor; ICS, inhaled corticosteroid; LABA, long-acting β2-agonist; MMAD, mass median aerodynamic diameter; MOC, micro-orifice collector; NGI, Next Generation Impactor; p10, p50 p90 10th 50th and 90th percentile inhalation curves; PIF, peak inspiratory flow; PIL, patient information leaflet; RH, relative humidity; SPC, summary of product characteristics; UPLC, ultra performance liquid chromatography

* Corresponding author.
E-mail address: farkas.arpad@energia.mta.hu (Á. Farkas).

http://dx.doi.org/10.1016/j.ijpharm.2017.09.057
Received 24 June 2017; Received in revised form 17 September 2017; Accepted 20 September 2017
Available online 21 September 2017

(e.g. De Boer et al., 2015) the NEXThaler® inhaler is a DPI (dry powder inhaler) device delivering an almost pressure-drop independent dose of BDP and FF. It has also been demonstrated that Foster® NEXThaler® emits a high fraction of fine (diameter < 5 μm) and extrafine (diameter < 2 μm) particles (Buttini et al., 2016) with high lung deposition efficiency and a more uniform deposition distribution (Mariotti et al., 2011). The special internal design and structure of the inhaler is considered to contribute to the above characteristics of the drug (Scichilone et al., 2013). The most innovative feature of the device is the built in BAM (breath-actuated mechanism). The BAM is a mechanical unit integrated into the NEXThaler® with the aim of delaying the emission of the drug until the flow rate of the patient is sufficiently high (about 35 L/min). This level flow rate causes high turbulence intensity inside the cyclone chamber, resulting in efficient detachment of drug particles from the carriers. The detachment is promoted also by the strong collisions between the particles with high kinetic energy and between the particles and the walls of the device (Corradi et al., 2014). While qualitatively the above reasoning seems to be logical and correct, a systematic quantitative analysis of the effect of the inclusion of BAM is still missing in the literature. A number of investigators have analysed by both Andersen Cascade Impactor (ACI) and Next Generation Impactor (NGI) the size distribution of drug particles emitted by NEXThaler® and proved that fine and extrafine particle fractions (FPF and EPF, that is, fractions of particles with aerodynamic diameter smaller than 5 μm and 2 μm, respectively, expressed as per cents of metered dose/label claim) are indeed high compared to the corresponding values of other DPI drugs in the market. Based on Table 1, which is a summary of the measurement results gathered from the open literature, the FPF is between 42.5% and 59.4% for BDP and between 43.3% and 56.7% for FF while the EPF is between 32% and 52.7% for BDP and between 22.5% and 48.9% for FF, depending on the flow rate of the impactor. The corresponding mass median aerodynamic diameter (MMAD) values were systematically low (between 1.1 μm and 1.7 μm).

However, it has not been analysed so far to what extent the advantageous aerodynamic characteristics of the emitted particles are due to the BAM. By the same token, the high number of the resulting fine and extrafine drug particles should lead to lower deposited upper airway doses and higher lung doses. To the best of our knowledge, an analysis on the effect of the presence of BAM on the amount of drug deposited in different regions of the airways is also missing. One way of studying the effect of BAM is to compute and compare the airway deposition distributions of the drugs emitted by the inhalers with BAM included and lacking it. Carefully validated numerical models proved to be a powerful tool in the quantification of total respiratory tract, regional and local deposition distributions of different drugs (e.g. Jókay et al., 2016; Horváth et al.,2017). However, most of the numerical models do not consider the growth of the inhaled particles due to the humid environment within the airways. Aerodynamic properties of the emitted aerosol drugs, like the parameters in Table 1, are also determined under certain humidity and temperature conditions. Knowledge of growth dynamics may be important also in the perspective of drug development. If drug particles are sufficiently small to enter the lungs and their hygroscopic growth is significant within particle residence time, then chances of exhalation decrease and lung deposition will be higher.

The main objective of this study is to apply experimental techniques to analyse the effect of the inclusion of BAM on the main aerodynamic characteristics of the emitted particles. Another aim is to use the measured values as inputs of numerical models to characterize the deposition distribution of the drugs in different anatomical regions of the airways and analyse the effect of BAM on the deposition of Foster® NEXThaler® drug. Finally, this study proposes to measure the hygroscopic growth of the drug particles emitted by NEXThaler® and to analyse the possible effect of their hygroscopic behaviour on the deposited drug dose distributions within the airways.

2. Methods

In this study both experimental techniques and numerical modelling tools were applied. Experimental measurements were performed to analyse the effect of BAM on the aerodynamic properties of the emitted particles. The results of these measurements were then used as inputs of the numerical airway deposition model. Extended hygroscopicity measurements of ICS and LABA drug components were also completed. Realistic breathing profiles of asthmatic patients through the NEXThaler® were used for both measurement and modelling purposes. The original inhalation profiles were acquired by Scuri et al. (2013) on 41 asthmatic patients with varying levels of disease control while they inhaled through the inhaler by using acoustic monitoring equipment. Casaro et al. (2014) then processed these profiles and calculated the p10, p50 and p90 representative profiles, which were adopted in our study. The p10, p50 and p90 curves were generated by calculating the 10th, 50th and 90th percentile cohort values at each recorded time interval (0.01 s). The p10, p50 and p90 inhalation profiles are characterised by 1.0 s, 1.9 s and 3.4 s inhalation times, and 45 L/min, 60 L/min and 100 L/min peak inspiratory flow (PIF) values, respectively. The three inhalation flow curves are plotted in Fig. 1.

We now present the experimental and numerical techniques used in this study.

2.1. Experimental method for the characterization of the emitted particles

The aim of experimental work was to measure and compare the particle characteristics emitted by NEXThaler® DPI inhalers with and

Table 1
Summary of the measured fine (< 5 μm) and extrafine (< 2 μm) particle fractions of the two drug components of Foster® NEXThaler® with different impactors at different flow rates retrieved in the open literature. FPF − fine particle fraction; EPF − extrafine particle fraction.

Impactor type	Flow rate (L/min)	FPF (% of label claim)		EPF (% of label claim)		Author
		BDP	FF	BDP	FF	
ACI	60	49.9	52.2	32.0	34.5	Zanker et al. (2011)
NGI	41.7	42.5	48.8	–	–	De Boer et al. (2015)
NGI	59	45.5	50.3	–	–	De Boer et al. (2015)
NGI	72.3	47.3	53.1	–	–	De Boer et al. (2015)
NGI	30	48.2	43.3	34.5	22.5	Buttini et al. (2016)
NGI	40	49.2	48.3	34.7	25.3	Buttini et al. (2016)
NGI	60	58.4	56.7	41.3	28.4	Buttini et al. (2016)
ACI	60	59.4	52.5	52.7	48.9	Buttini et al. (2016)
NGI	90	57.9	56.7	43.4	34.9	Buttini et al. (2016)
NGI	realistic profile, p10	45.9	45.3	36.4	30.8	Casaro et al. (2014)
NGI	realistic profile, p50	48.8	48.3	38.9	32.7	Casaro et al. (2014)
NGI	realistic profile, p90	47.4	44.5	36.8	28.8	Casaro et al. (2014)

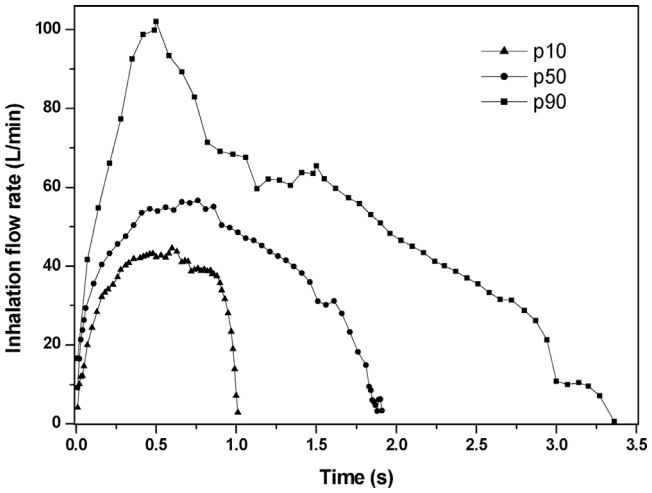

Fig. 1. *In vivo* 10th, 50th and 90th percentile inhalation curves (p10, p50 and p90 profiles) of asthmatic patients adopted from Casaro et al. (2014).

without BAM, and to provide realistic inputs for the airway deposition model.

The inhalation profiles in Fig. 1 were implemented into the Copley BRS 3000 Breath Simulator Model to apply realistic characteristic breathing profiles in the *in vitro* aerosol performance analysis experiments. This breathing simulator was part of our experimental setup also containing an NGI demonstrated in Fig. 2.

A NEXThaler® (Lot 1043523 Exp 04/2019) was opened from its foil pouch and rested for a minimum of 96 h at 25 °C and 70% RH before testing to allow any antistatic charge to dissipate. Prior to any analysis, five waste shots were actuated from the devices into a waste dosing unit sampling apparatus (DUSA) set at 60 L/min. The use of five shots was considered appropriate to ensure the necessary response of the detector that was used to analyse the formoterol fumarate (the component with the lowest mass) within the test samples. The device was weighted (readability 0.01 mg) before and after each shot to ensure dose evacuation. The NEXThaler® device was analysed using all three inhalation profiles in Fig. 1. In order to characterize the aerosol cloud in the NGI a steady state volumetric flow rate was set at values relative to the peak values reached in the various inhalation profiles (45 L/min for p10, 60 L/min for p50 and 100 L/min for p90). This is possible due to the incorporation of the Copley 'flow splitter' into the system, located in-between the Pre-separator and Throat. When the system is 'balanced' the Copley BRS 3000 is used to generate the inhalation profile that is drawn in through in the inhaler and throat assembly. All NGI measurements were conducted in triplicate and each test replicate was based on five separate doses being delivered from each NEXThaler® device. Additionally, the assessments were performed in a non-consecutive order. The NEXThaler® device was weighed before and after each actuation to estimate the shot weight (mg). Samples were collected from the throat, pre-separator and the NGI stages, and analysed for BDF/FF content. A suitable solvent mixture of acetonitrile (ACN): buffer (45:55) was used to collect and dissolve the samples. Test samples were analysed by Acquity Ultra Performance Liquid Chromatography (UPLC) with Photodiode Array Detector (PAD, Waters, Wilmslow UK), ACE Excel C18 Amide 100 × 2.1, 2 µm Column (Hichrom, UK), with an injection volume of 10 µL and a flow rate of 0.75 mL/min. External standard solutions for formoterol fumarate (0.04 µg/ml sensitivity check, 4 µg ml/1 calibration standard and 4 µg ml/1 verification standard), gradient method with a run time of 8 mins (Line A: 90:10 buffer: acetonitrile and Line B: 10:90 buffer: acetonitrile). The gradient use was Line A = 100% at 0 min, 66% at 4 min, 25% at 7 min and 100% at 7.1 min. The UPLC procedure was verified for specificity, linearity, reproducibility and system suitability. The device retention could not be measured for the NEXThaler®, however it was possible to measure the change in mass. In order to test the device without a BAM a thin spatula was used to trigger the BAM before firing the device. This was achieved by inserting the spatula through the air inlet vents located on top of the NEXThaler® and pushing downwards on the BAM flap to release the spring, opening the dose protector.

Fig. 2. Experimental setup including the NGI impactor and BRS 3000 breathing simulator.

2.2. Measuring the hygroscopic growth dynamics of pharmaceutical aerosol

The relationship between the diameter of an aerosol droplet and the relative humidity (RH) is important to accurately parameterize in any lung inhalation model; the dynamic behaviour of the aerosol size during inhalation can be expected to have a significant effect on where the dose is delivered (Haddrell et al., 2014). Here, we report the hygroscopic properties of various pharmaceutical aerosols measured using a single particle analysis technique termed the comparative kinetic electrodynamic balance (CK-EDB). A detailed explanation of this technology has been reported previously (Rovelli et al., 2016; Davies et al., 2013), and only a brief description will be given here (Fig. 3).

The reservoirs of two droplet-on-demand dispensers were filled and positioned such that droplets could be injected directly into the trap, one with a starting solution containing the pharmaceutical at a known concentration and the other with pure water (Fig. 3, left). As a droplet is dispensed, a slight charge (< 5 fC) is imparted by the placement of an induction electrode held at a fixed DC bias close to the dispenser; the presence of this charge enables the droplet to be strongly trapped by the electrodynamic fields of the trap. Once trapped, the radius of the droplet is probed by measuring the angularly dependent light scattering (the phase function) from an incident laser at 532 nm. The phase function is compared with simulations from Mie scattering theory to infer the droplet radius. During the drying process of all the pharmaceuticals, the particles did not reach a water activity low enough to form an amorphous solid as evidenced by the coherence of the phase function. The phase function is measured at a frequency of 100 Hz until the droplet reaches an equilibrium with the RH of the airflow, achieving a steady aqueous liquid droplet size. Through sequentially trapping droplets originating from the two dispensers, accurate estimations of the water activity of the airflow that the pharmaceutical containing droplet evaporates into can be inferred by the mass flux from the water droplet (Davies et al., 2013).

At any moment in time during the droplet evaporation, the mass flux of water from the droplet is dependent on the instantaneous water activity which is dependent on the solution composition; this relationship has been reported by Kulmala et al. (1993), and is used to convert CK-EDB measurements to hygroscopic growth curves (Rovelli et al., 2016). The relationship between mass flux and water activity is shown in Eq. (1):

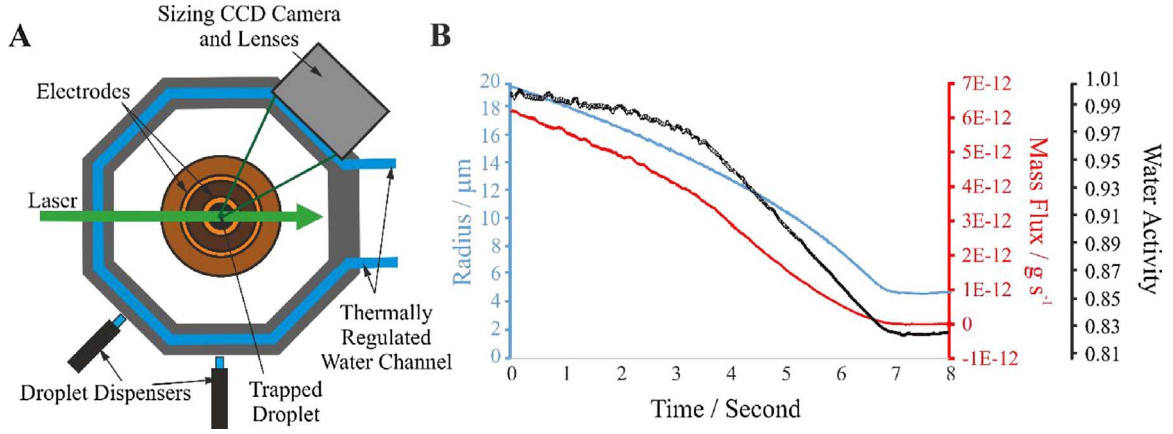

Fig. 3. (A) Experimental setup of the CK-EDB. (B) From the dynamic behaviour of an aqueous lactose solution droplet injected into an airflow with an RH of 83%, the water activity of the droplet at each moment in time can be calculated from the mass flux from the droplet.

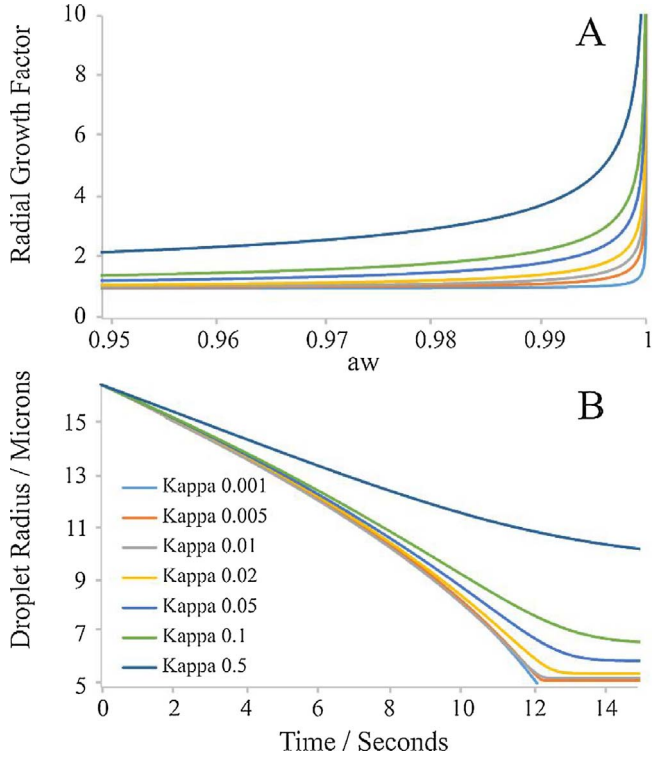

Fig. 4. (A) The radial growth factor of various organic species as a function of κ. (B) The dynamic behaviour of a single droplet injected into an airflow with an RH of 92% where the starting solution is an organic with a given κ value whose concentration is 13 g/L.

Table 2
Times elapsed from the beginning of inspiration until the aerosol bolus starts, reaches its maximum and ends at p10, p50 and p90 flow profiles in case of devices including a BAM and without it.

Device	Inh. profile	Start (s)	Peak (s)	End (s)	Duration (ms)
NEXThaler® with BAM	p10	0.44	0.49	0.60	164
	p50	0.35	0.40	0.52	170
	p90	0.30	0.35	0.48	180
NEXThaler® without BAM	p10	0.18	0.26	0.35	170
	p50	0.20	0.27	0.37	170
	p90	0.20	0.27	0.44	239

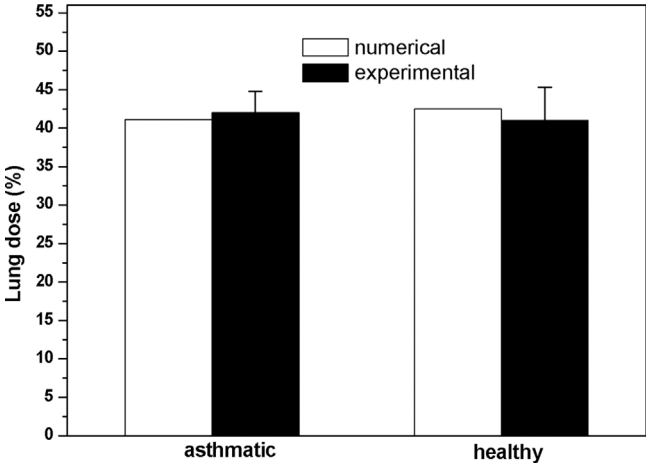

Fig. 5. Comparison of simulated lung doses of asthmatic patients and healthy individuals expressed as percent of nominal emitted dose with lung dose values of Mariotti et al. (2011) measured by scintigraphic methods.

$$I = 4\pi a(S_\infty - S_a)\left[\frac{RT_\infty}{M\beta_M Dp_e(T_\infty)A} + \frac{S_a L^2 M}{R\beta_T KT_\infty^2}\right]^{-1} \quad (1)$$

where I is the mass flux of evaporating water and a is droplet radius. S_a is the fractional saturation vapour pressure (equivalent to the water activity in the droplet) at the specific composition of the droplet at each moment in time. S_∞ is the water activity of the airflow (as measured by the probe water droplet), T_∞ is the gas phase temperature, M is the molecular mass of water, L is latent heat of evaporation, the transitional correction factors are β_M and β_T for mass and heat transfer, D is vapour diffusion coefficient, $p_e(T_\infty)$ is pressure, K is the thermal conductivity of the gas phase, and A is Stefan flow correction.

Thus for an evaporating droplet (Fig. 3B), at each point in time the mass flux from the droplet can be used to calculate the fractional saturation vapour pressure S_a (the water activity); every other quantity in equation 1 is known, measurable or can be calculated. Since the starting concentration and radius of the droplet is known, a dry radius of the droplet can be calculated. From the ratio of the absolute radius of the droplet at each moment in time to the dry radius, the radial growth factor is readily calculated, providing a size-independent method for representing the level of hygroscopic growth for the aerosol. This approach was used in this publication to determine the hygroscopic growth of NaCl and lactose (the carrier in Foster® NEXThaler®).

For highly insoluble species (such as BDP and FF) a slightly different approach was taken. Insufficient solute could be dissolved in water alone to yield an evaporation curve with changing mass flux similar in

Table 3
Mass of BDP and FF deposited in the throat (THR), preseparator (PRE), on different stages (S1-S7) of the impactor and in the micro-orifice collector (MOC).

Flow	Stage	Size range (μm)	Deposited dose (μg)				Standard deviation (μg)			
			BAM		no-BAM		BAM		no-BAM	
			BDP	FF	BDP	FF	BDP	FF	BDP	FF
p10	THR	> 17.3	12.340	0.617	12.176	0.658	1.024	0.044	0.881	0.083
p10	PRE	13.9–17.3	27.540	1.515	50.559	3.016	2.834	0.139	1.459	0.073
p10	S1	9.41 – 13.9	0.251	0.027	0.520	0.043	0.036	0.002	0.004	0.003
p10	S2	5.18 – 9.41	1.159	0.063	1.813	0.104	0.090	0.003	0.045	0.018
p10	S3	3.26 – 5.18	3.120	0.167	3.047	0.157	0.226	0.022	0.364	0.005
p10	S4	1.9 – 3.26	5.480	0.495	4.629	0.337	0.441	0.043	0.212	0.007
p10	S5	1.09 – 1.9	7.668	0.647	4.303	0.337	0.904	0.070	0.244	0.006
p10	S6	0.65 – 1.09	7.960	0.481	3.217	0.192	1.136	0.067	0.118	0.009
p10	S7	0.41 – 0.65	3.841	0.204	1.451	0.095	0.301	0.014	0.282	0.009
p10	MOC	< 0.41	9.253	0.440	3.735	0.177	0.441	0.016	0.343	0.023
p50	THR	> 14.4	13.042	0.657	14.404	0.802	0.903	0.082	1.406	0.090
p50	PRE	12.8–14.4	28.365	1.633	46.257	2.738	0.632	0.130	1.875	0.129
p50	S1	8.06 – 12.8	0.555	0.046	0.891	0.066	0.131	0.012	0.119	0.007
p50	S2	4.46 – 8.06	1.977	0.110	2.452	0.131	0.181	0.011	0.042	0.004
p50	S3	2.82 – 4.46	4.411	0.305	3.749	0.224	0.337	0.038	0.297	0.022
p50	S4	1.66 – 2.82	6.998	0.693	4.790	0.417	0.227	0.041	0.749	0.053
p50	S5	0.94 – 1.66	8.124	0.665	4.120	0.323	0.124	0.023	0.753	0.059
p50	S6	0.55 – 0.94	7.154	0.426	2.794	0.176	0.101	0.025	0.298	0.020
p50	S7	0.34 – 0.55	4.289	0.241	2.041	0.129	0.085	0.008	0.971	0.062
p50	MOC	< 0.34	10.315	0.486	3.676	0.167	0.081	0.004	0.886	0.044
p90	THR	–	13.320	0.760	13.801	0.775	0.270	0.035	1.444	0.167
p90	PRE	> 9.7	25.120	1.534	43.978	2.593	0.990	0.224	1.370	0.021
p90	S1	6.12 – 9.7	1.476	0.082	1.828	0.117	0.256	0.016	0.280	0.004
p90	S2	3.42 – 6.12	3.793	0.246	3.366	0.194	0.135	0.019	0.308	0.017
p90	S3	2.18 – 3.42	6.027	0.553	4.253	0.353	0.191	0.018	0.459	0.036
p90	S4	1.31 – 2.18	7.584	0.771	5.117	0.464	0.308	0.013	0.974	0.101
p90	S5	0.72 – 1.31	7.323	0.538	4.277	0.299	0.381	0.021	0.593	0.036
p90	S6	0.4 – 0.72	5.299	0.327	2.902	0.176	0.047	0.017	0.788	0.025
p90	S7	0.24 – 0.4	3.982	0.237	1.995	0.121	0.056	0.031	0.442	0.008
p90	MOC	< 0.24	9.279	0.390	5.214	0.228	0.899	0.046	1.215	0.075

profile to that in Fig. 3B; a saturated aqueous solution of the insoluble species was often so low in concentration that the evaporation curve had an appearance that resembled the evaporation of a pure water droplet. Instead, a more concentrated solution of the insoluble species was prepared in ethanol and injected into the trap at elevated RH (as high as 95%) in a similar way to the earlier measurements. The rapid loss of ethanol and condensation of water led to the equilibration of an aqueous solute droplet with a much higher solute mass and larger size than could be achieved by dissolving straight in water. Then, based on the known mass of solute derived from the size of the original ethanol droplet, the approach to an equilibrium size in the evaporation profile at times close to 10 s could be compared with simulations of the expected profiles for droplets of varying hygroscopic response. For convenience, κ-Kohler theory was chosen to represent the simulated form of the hygroscopic thermodynamic response; this theory is extensively used in aerosol science to reduce the hygroscopic response to a single number, the value of κ (Petters and Kreidenweis, 2007). In these cases, the relationship between radial growth factor (*GF*) and water activity (a_w) is estimated from the relationship:

$$RadialGrowthFactor = GF = \frac{DropletRadius(a_w)}{DropletRadius(Dry)} = \sqrt[3]{1 + \frac{ka_w}{1 - a_w}} \quad (2)$$

Fig. 4A shows the functional forms of Eq. (2) for different values of κ. The simulated change in the time-dependence of the size during evaporation to changes in κ is shown in Fig. 4B. Although not providing a comprehensive representation of the thermodynamics, if the measured evaporation profiles close to equilibration in size are compared and related to the initial composition, then the time-dependent profiles can be used to differentiation between particles of differing κ values. Thus, by using this approach it was possible to establish an upper limit of hygroscopic growth, i.e. an upper limit on κ. For a more extensive description of this technique, refer to the Supplementary information.

2.3. Description of the computational method

The numerical model used in this work is a stochastic whole airway deposition model. The inputs of the model are the parameters related to breathing and drug particles, while the output can be the whole respiratory tract, regional (e.g. upper airways, bronchial airways, acinar airways), lobar, or airway generation number specific deposition fractions. The model was initially developed by Koblinger and Hofmann (1990). In this study the model has been adapted and validated for the case of medical aerosols. Upper airway deposition of the inhaled aerosol drugs is computed based on empirical deposition formulas of Cheng (2003). The asymmetrical geometry of the bronchial and bronchiolar airways is based on the statistical analysis of morphometrical data published by Raabe et al. (1976). Airway lengths and diameters, and branching and gravity angles are selected by Monte Carlo techniques. The acinar part is constructed based on the information retrieved in the work of Haefeli-Bleuer and Weibel (1988). Deposition of the inhaled particles in each conducting airway generation is computed based on theoretical formulas of gravitational settling, inertial impaction and thermal diffusion valid for straight and bent tubes. The same deposition mechanisms are accounted for in the region of acinar airways. The model is able to handle any particle size distribution and track the particles inhaled uniformly during the inspiratory phase, but also inhaled as an aerosol bolus. Pasquali et al. (2015) has demonstrated that the fluidisation event is very short and the drug is released from the NEXThaler® within 0.1–0.2 s. Tweedie and his co-workers (Tweedie et al., 2015; Tweedie and Lewis, 2016) performed optical measurements and deduced the starting time, time of the peak intensity and duration of the aerosol bolus emitted by the NEXThaler® devices with and without a BAM. The measured values, which were implemented

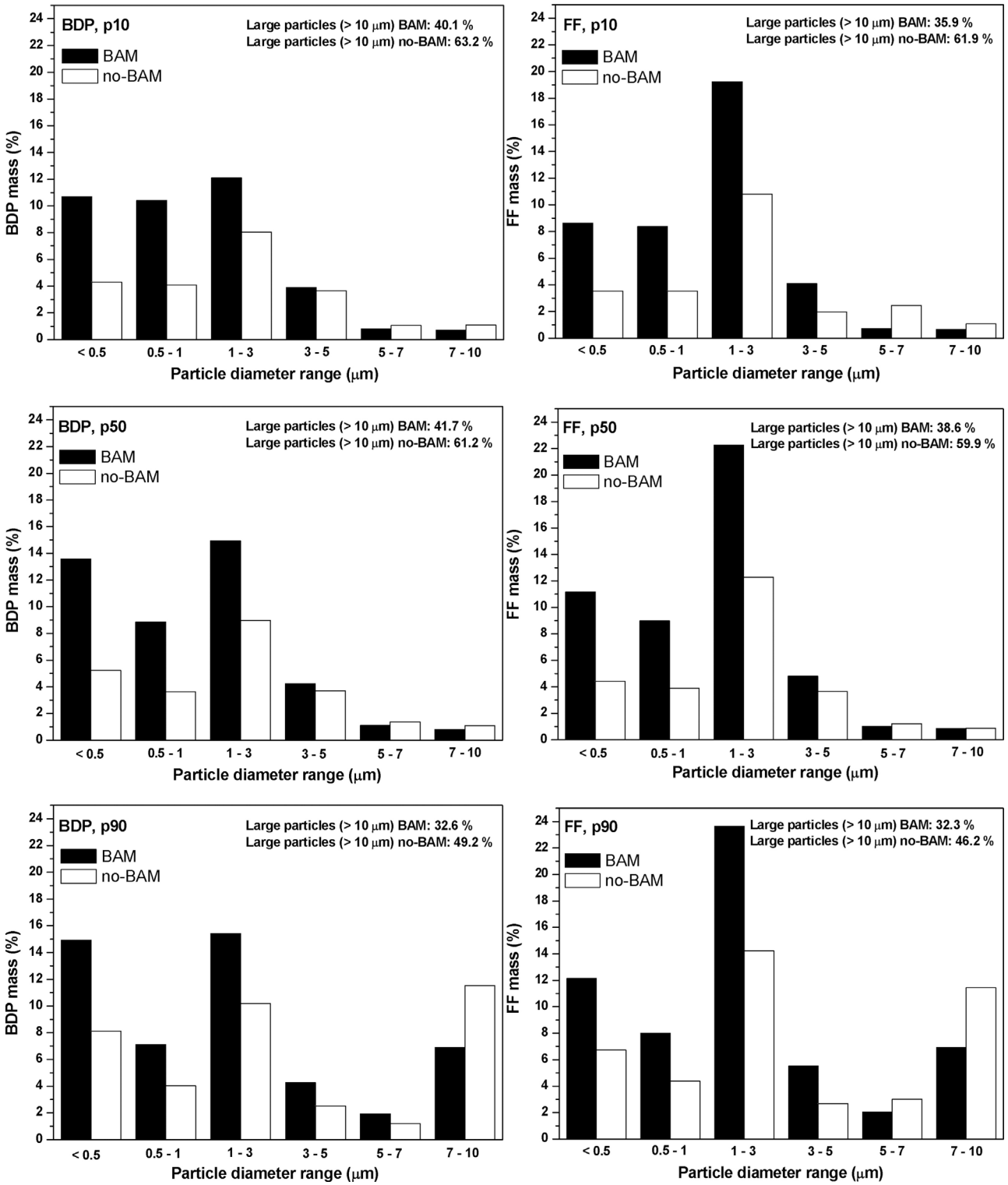

Fig. 6. Size distributions of BDP (left panels) and FF (right panels) drug components originating from NEXThaler® inhalers with BAM and without BAM corresponding to p10 (upper panels), p50 (middle panels) and p90 (bottom panels) inhalation profiles. All values are expressed as a percent of metered dose. The figure shows the mean values for 3 inhalers and 5 shots/inhaler.

into the numerical model, are summarized in Table 2.

Contrary to the most of current particle deposition models, our model can be applied also in case of asymmetrical breathing cycles and breathing patterns containing breath-holds. A recent major development of the model regarded the implementation of algorithms aiming at computing the deposition based on the realistic breathing curve. Earlier versions dealt with constant inspiratory and expiratory flow rates based on the inhaled/exhaled volume and inhalation and exhalation times. The deposition model has been earlier validated based on experimental scintigraphic deposition data (see Farkas et al., 2016). Since in this work the model was applied to compute the deposition of Foster® NEXThaler® drug particles, present validation process consisted in comparing our theoretical deposition results with deposition data of Foster® NEXThaler® yielded by the scintigraphic experiments of Mariotti

Table 4
Shot weight, delivered dose (DD), fine particle dose (FPD) and fine particle fraction (FPF) values with standard deviations of BDP and FF drug components emitted by NEXThaler® inhalers with and without BAM corresponding to p10, p50 and p90 inhalation profiles.

	BAM						no-BAM					
	p10		p50		p90		p10		p50		p90	
	BDP	FF	BDP	FF	BDP	FF	BDP	FF	BDP	FF	BDP	FF
Shot weight (mg)	8.6 (0.3)	8.6 (0.3)	8.8 (0.4)	8.8 (0.4)	8.6 (0.4)	8.6 (0.4)	9.0 (0.4)	9.0 (0.4)	8.8 (0.2)	8.8 (0.2)	8.8 (0.2)	8.8 (0.2)
Delivered Dose (μg)	78.6 (5.7)	4.7 (0.3)	85.2 (2.3)	5.3 (0.3)	83.2 (3.4)	5.4 (0.4)	85.5 (0.1)	5.1 (0.1)	85.2 (2.6)	5.2 (0.2)	86.7 (2.1)	5.3 (1.8)
Fine Particle Dose (μg)	37.2 (3.4)	2.4 (0.2)	41.9 (0.9)	2.8 (0.1)	42.4 (1.9)	3.0 (0.2)	20.2 (0.5)	1.3 (0.0)	21.8 (3.4)	1.5 (0.2)	26.2 (2.2)	1.8 (0.2)
Fine Particle Fraction (%)	47.3 (1.8)	52.1 (1.9)	49.1 (0.3)	54.2 (1.3)	50.9 (0.2)	55.3 (1.6)	23.6 (0.6)	25.1 (0.6)	25.6 (3.8)	28.4 (4.2)	30.2 (1.8)	33.5 (2.1)

et al. (2011). The outcome of this comparison can be seen in Fig. 5. As the figure demonstrates the modelling results are in good agreement with the measurements performed for similar input data values. The differences between the measured and simulated lung doses are lower than the uncertainties of the measurements shown by the error bars. The good agreement between the calculated and experimentally determined deposition values indicates that our model is suitable for the simulation of Foster® NEXThaler® deposition.

3. Results

The results of the NGI measurements of BDP and FF masses emitted by NEXThaler® inhalers with and without BAM corresponding to the inhalation profiles in Fig. 1 are presented in Table 3. The measurement errors corresponding to the measured quantities are demonstrated as well. The size intervals corresponding to the throat, preseparator, impactor stages and MOC (micro-orifice collector) are also provided. The cut-off diameter values of the throat and prseparator were derived from the works of Roberts et al. (2000), Zhou et al. (2011), Marple et al. (2003) and Cheng et al. (2015).

It is worth noting that since the flow rates are different in the case of p10, p50 and p90 profiles, different cut-off diameters correspond to stages with the same name. In addition, the cut-off diameters of the throat and pre-separator are also flow rate dependent. To facilitate the interpretation of size distributions at different flow rates, and later their effect on airway deposition distribution, the results in Table 3 were processed to represent all size profiles using the same size bins. These profiles are presented in Fig. 6. As Fig. 6 demonstrates the inhaler containing a BAM emits significantly lower number of large particles and higher number of small particles. The mass of drug emitted and deposited in the preseparator by the NEXThaler® was determined to be 32 ± 3% (with BAM) and 54 ± 4% (without BAM). Thus, significantly more drug mass was found to reach the cascade impactor stages associated with therapeutic dose when the BAM was present.

The role of BAM is to delay the release of powder until the flow velocity is sufficiently high. This high flow rate leads to high turbulence intensity in the cyclone chamber. Inhaled air enters this part of the inhaler and forms a cyclonic flow. Turbulent airflow and particle-wall collisions lead to both powder de-aggregation and release of active substance detachment from the carriers. These observations are reflected in the higher fine particle fractions emitted by the NEXThaler® with BAM. The exact values of fine particle fractions are presented in Table 4 together with the shot weights, delivered doses and fine particle dose values. Based on Table 4 the FPF of BDP varies between 47 and 51% if the BAM is present and between only 24–30% if the BAM is missing. Similarly, the FPF of FF takes values between 52 and 55% if the with BAM included and between only 25–34% without BAM. The significantly higher FPF values obtained for the inhaler with BAM indicates a potential for higher lung depositions.

To quantify the expected increase of lung deposition the numerical model described in the Methods section has been applied. Fig. 7 depicts the BDP (left panels) and FF (right panels) deposited extrathoracic and lung doses in case of p10 (upper panels), p50 (middle panels) and p90 (bottom panels) inhalation profiles for the inhalers with BAM and without BAM, expressed as a percent of metered dose. As it can be observed in the panels of Fig. 7, deposited upper airway and lung doses do not sum up to 100%. The remaining fraction corresponds to the exhaled fraction (emitted dose demonstrated in Table 4 minus total airway dose presented in Fig. 7) and the dose fraction deposited in the device (metered dose or label claim minus emitted dose).

Since the patient information leaflet (PIL) of Foster® NEXThaler® advices 5 s to 10 s of breath-hold after the inhalation of the drug, the results in Fig. 7 refer to these two reference breath-hold time (BH) values. As a general tendency, for every inhalation profile the upper airway dose decreased and the lung dose increased by the inclusion of BAM, except the BDP deposition at p10 for the lower breath-hold time. The upper airway deposition of BDP decreased from about 60% to about 40%, while the FF deposition in the same region decreased from about 60% to 35–40% for the inhaler with BAM compared to the inhaler with no-BAM. Nevertheless, extrathoracic deposition of the drug emitted by the same inhaler (with BAM or without BAM) remained relatively unchanged for the three flow profiles. Deposition in the ET region is mostly due to inertial impaction, which increase with both the increase of particle size and air velocity. In the present case particle velocities increase from p10 to p50 then towards p90, but particle diameters (masses) decrease. ET deposition is a result of the two competing tendencies. At the same time, the lung dose of BDP increased mostly for the p50 (from 19–21% to 30–38%) and p90 (from 25–26% to 39–41%) profiles. By the same token, lung deposition of FF increased from 21–23% to 38–39% at p50 and from 28–30% to 46–48% at p90 profile. All deposition values are expressed as a percent of the metered dose (label claim).

Based on our experiments, hygroscopic growth of drug particles can be important. The hygroscopic response of saline (NaCl), lactose (micronized LH300), BDP and FF were measured using the CK-EDB and are presented in Fig. 8. While full hygroscopic response curves were measured for saline and lactose, the hygroscopic response of BDP and FF were estimated from the shape of the limiting behaviour on approaching equilibrium and comparison with the simulated evaporation curves for droplets of varying κ. The low values of κ for these compounds are consistent with highly insoluble compounds (Petters and Kreidenweis, 2007).

To demonstrate the effect of hygroscopic growth on drug airway deposition the lung deposition values for p10 profile were recalculated by considering the hygroscopic changes in particle diameters. To cover the whole size distributions measured by the impactor for the p10 profile (Fig. 6, upper panels) nine different initial diameter values were considered (0.3 μm, 0.5 μm, 0.9 μm, 1.5 μm, 2.6 μm, 4.3 μm, 7.3 μm,

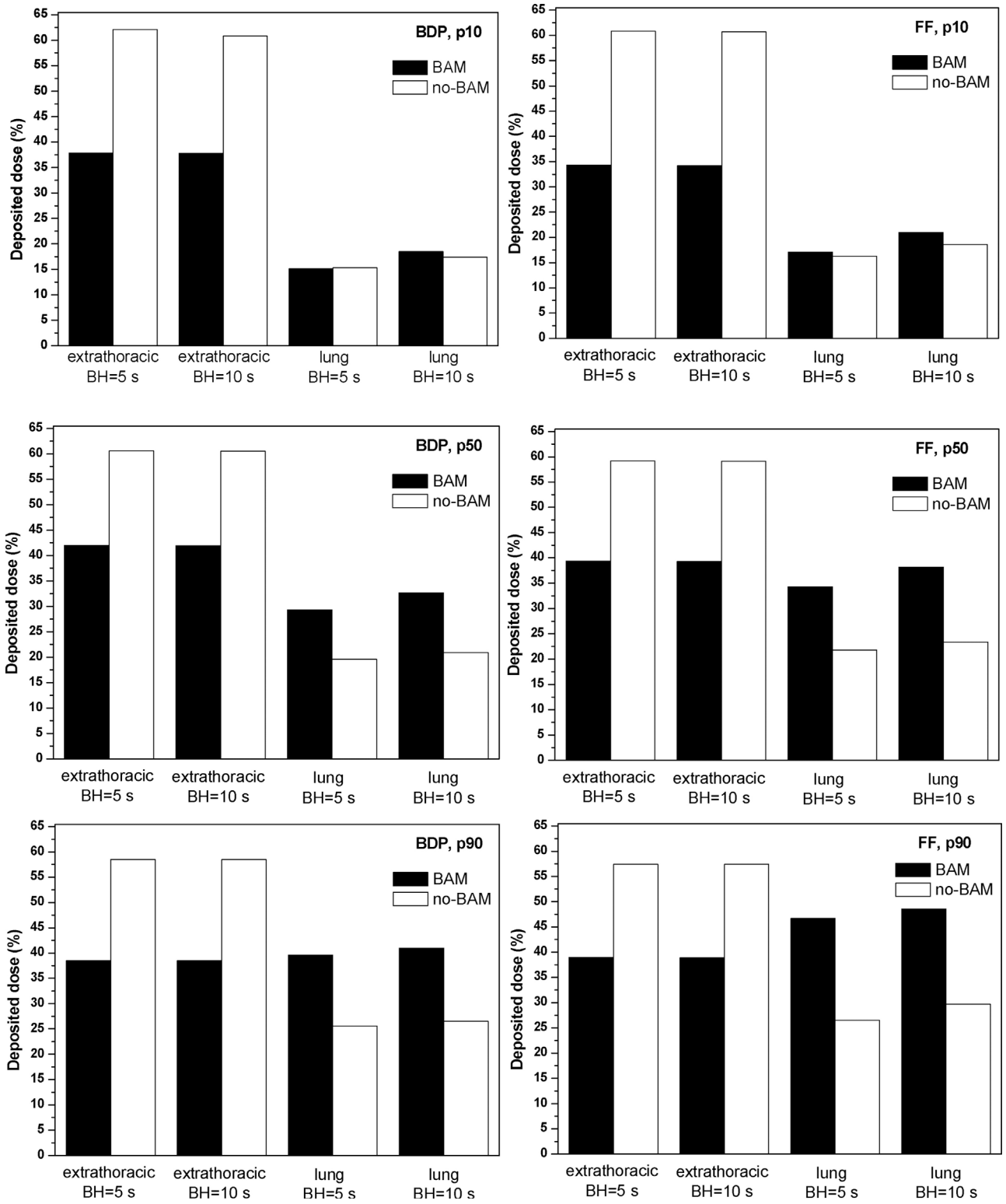

Fig. 7. Comparison of BDP (left panels) and FF (right panels) deposited extrathoracic and lung doses in case of p10 (upper panels), p50 (middle panels) and p90 (bottom panels) inhalation profiles assuming 5 s and 10 s breath-hold times (BH) for the inhalers with BAM and without BAM, expressed as a percent of metered dose.

11.7 μm, 15 μm). Fig. 9 shows the post-inhalation time dependence of the diameters of FF, BDP and lactose particles with given diameters at the moment of inhalation. Note that particle size at inhalation depends on the RH the particle is in equilibrium with prior to inhalation. For the sake of simplicity, in the following sample calculations it was considered that at inhalation RH = 50%, similar to the value characteristic of the laboratory environment during the size distribution measurements. For other values of RH at inhalation the measured size distribution can be converted by first determining the dry (RH = 0%) size distribution, then computing the sizes for the corresponding non-zero RH value. Table 5 reports the dry diameters of the particle sizes considered at RH = 50%.

Taking into account hygroscopic growth of particles shown in Fig. 9, lung deposition of Foster® NEXThaler® at p10 profile changes compared

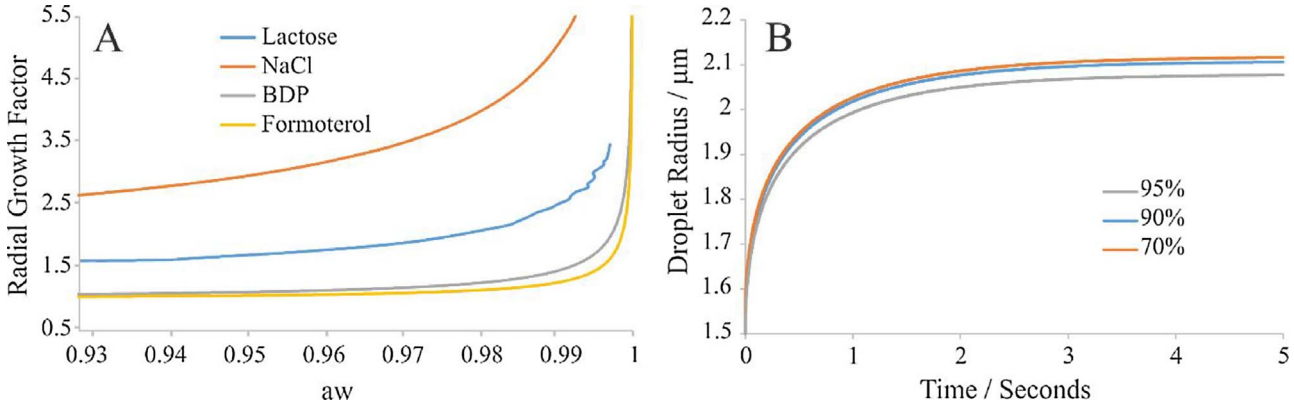

Fig. 8. (A) Summary of the hygroscopic behaviour of soluble and highly insoluble pharmaceutics measured. The value of κ for FF is 0.01 (+/− 0.005) and for BDP is 0.02 (+/− 0.005) while the radial growth factors for NaCl and Lactose were measured from the mass flux. (B) Based on the hygroscopic growth measurements, simulations of the growth kinetics of the radius of an FF droplet with initial diameter of 1.5 µm. Calculations are shown at three different starting relative humidities with the droplet at equilibrium prior to inhalation (0 s corresponds to the moment of inhalation). RH in the airways is 99.5%.

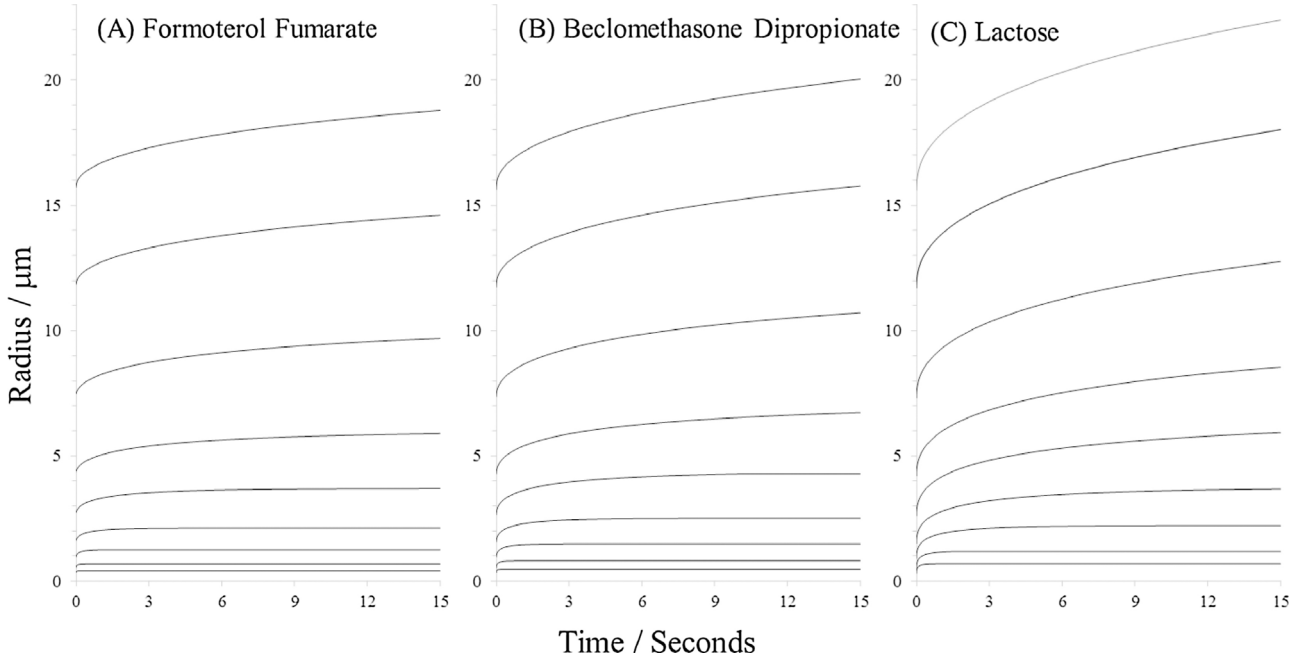

Fig. 9. Hygroscopic growth of FF (panel A), BDP (panel B) and lactose (Panel C) particle diameters after the inhalation assuming ambient RH value of 50% and lung RH value of 99.5%.

to that demonstrated in Fig. 7 (upper panels). The new values are depicted in Fig. 10. The figure demonstrates that the existence of BAM leads to the increase of lung dose even for the weakest inhalation profile (p10), which was not obvious without considering the hygroscopic growth of drug particles. Actually, the differences in Fig. 10 are the result of three major factors. Indeed, size distribution differences between BAM and no-BAM are evident even for the lowest studied inhalation strength causing lower upper airway and higher lung deposition when BAM is present. However, this effect is counterbalanced by the fact that in no-BAM case particles are released sooner and have more chances to penetrate deeper and more time to deposit by gravitational settling. Actually, these two competing mechanisms are at play also for the higher flow rates, but there the release of particles happens earlier (see Table 2) even with BAM and the inhaled volume is also higher, thus small particles have more chances to reach the lungs. What Fig. 10 intends to highlight is the effect of the third factor, that is, hygroscopic growth. By this effect particles which were small enough to enter the lungs become larger and deposit more efficiently by impaction (which is not time dependent).

Table 5
Dry diameters of BDP and FF particles corresponding to their RH = 50% diameters.

Diameter at RH = 50% (µm)	Diameter at RH = 0% (µm)	
	BDP	FF
0.3	0.30	0.30
0.5	0.50	0.50
0.9	0.89	0.90
1.5	1.49	1.50
2.6	2.58	2.59
4.3	4.17	4.19
7.3	7.25	7.28
11.7	11.62	11.66
15.6	15.50	15.55

4. Discussion

Regardless to the inhalation profile used, an increased fraction of

both BDP and FF is observed in the pre-separator when the BAM is pre-triggered by the analyst. This corresponds to a reduced NGI stage deposition and consequently a lower fine particle dose. With the BAM present, the fine particle dose is greatly improved, less material is found in the pre-separator, more in the lower stages with a noticeable increase in MOC. This effect is likely to be due to the increased entrainment air velocity caused by the delayed entrainment and dispersion of the formulation when the BAM is present. Indeed, earlier works have demonstrated that the NEXThaler® device starts emitting the drug when the flow rate of the patient reaches a value of about 35 L/min (Corradi et al., 2014; Pasquali et al., 2015; Mason et al., 2015). The higher flow-rate means higher air velocity, thus higher turbulence intensity inside the cyclone chamber. In addition, particle-particle and particle-device wall collisions are more powerful. As a consequence, the detachment of drug particles from the carriers is more efficient and more small particles are emitted from the device. Present numerical computations demonstrated that the higher FPF translates into lower upper airway doses and higher deposited doses in the lungs. In this way, the probability of the unwanted side effects decreases and the likelihood that the drug reaches the receptors increases. In this work the clinical effect was not investigated, however, increased lung deposition most probably contributes to a more efficient therapy. The only exception from the tendencies described above was the case of p10 profile, where the lung doses corresponding to the BAM and no-BAM cases are about the same (Fig. 7, upper right panel). The explanation for this apparent exception is the presence of two competing effects. The first effect is related to the inhaled particle size distribution and the second to the inhalation time of the particles. With regards to the p10 inhalation profile, particles penetrate deeper into the lungs when no BAM is present. This is because the aerosol bolus is emitted earlier from the inhaler; i.e. prior to the pressure drop required to trigger the BAM. If the particles are small (< 3 μm) deposition within the respiratory tract is dominated by sedimentation and diffusion within the deep lung. However, deposition by sedimentation and diffusion is less dominant for larger particles which mainly deposit by impaction in the oropharynx and bronchi, i.e. prior to reaching the lungs. It therefore follows, that total lung deposition is a function of the inhaled particle size distribution and the point at which the particles are inhaled. For the higher capacity inhalation profiles p50 and p90 sedimentation and diffusion are predominant and lung deposition is increased when the BAM is present. For the lower capacity inhalation profile, p10, a small amount of air is slowly inhaled (about 0.6 L). Thus for the p10 case, particles, which are emitted in a later phase of the inhalation (from 0.44 s in the BAM case) will not enter the deeper regions of the lung and sedimentation and diffusion mechanisms will be less significant. As a result, the observed advantages of the BAM with inhalation profiles p50 and p90 are less evident for the p10 inhalation profile.

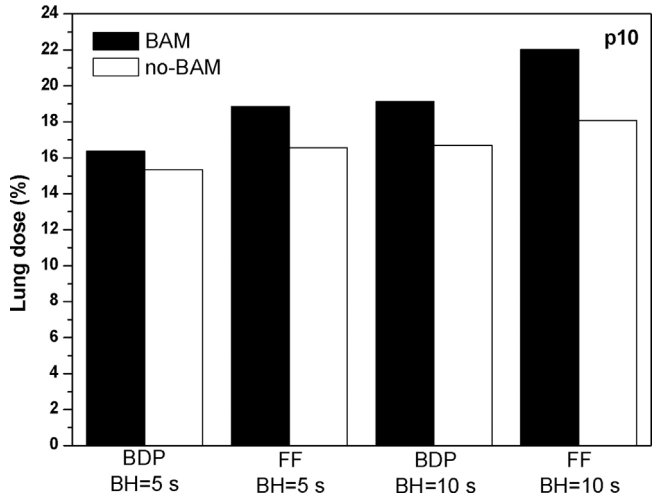

Fig. 10. Lung doses of hygroscopic BDP and FF drug components in case of p10 inhalation profile assuming 5 s and 10 s breath-hold times (BH) emitted by inhalers with BAM and without BAM, expressed as a percent of metered dose.

Finally, all the results in Fig. 7 may be affected by particle hygroscopicity. If hygroscopic growth is relevant, then particle sizes shift towards higher diameter values and the second effect mentioned above is not so powerful. As a result, the BAM case yields higher lung deposition even for p10 inhalation flow profile (Fig. 10). Indeed, present hygroscopicity measurements yielded κ values of 0.010 ± 0.005 for FF and 0.020 ± 0.005 for BDP of a 1.5 μm particle (comparable to the measured values of FF and BDP MMADs), which at RH = 99.5% translates into radial growth factors of 1.4 and 1.7, respectively. Time scales of inhalation and exhalation plus a 5–10 s breath-hold brings us into the region where hygroscopic growth factors are relevant. Indeed, the results depicted in Fig. 10 clearly demonstrate that considering realistic hygroscopic growth leads to higher lung depositions of BDP and FF for the inhalers with BAM than for the inhalers without BAM for both 5 s and 10 s breath-hold times even for the weakest inhalation profile (p10). This result emphasizes the importance of measuring the hygroscopic behaviour of all the marketed drugs and drug components but also the necessity of the inclusion of the hygroscopic effect into the numerical deposition models in the future.

5. Conclusions

As inhaler devices become more sophisticated and development of connected smart inhaler devices become publicised (Chan et al., 2015), the NEXThaler® remains a relatively new device with several innovative, yet non-electronic, features. In particular, a breath actuated mechanism (BAM) has been incorporated into the design. To the best of our knowledge the present work is the first systematic study regarding the effect of this mechanism on the airway deposition of Foster® NEXThaler®. Based on the results of this study the BAM leads to; a reduction in the large particles emitted; lower upper airway deposited doses; an increase in the available therapeutic fine particle fraction (FPF); resulting in a significantly higher lung dose. The observations from our study suggest inclusion of the BAM provides an improved clinical outcome. This work has also demonstrated that hygroscopicity may play an important role in lung deposition. Knowledge of particle growth dynamics, particle residence times within different regions of the airways and deposition distributions may lead to a more intelligent drug development in the future to decrease upper airway drug deposition and increase it in the targeted regions.

Author disclosure statement

None of the authors have shares in any pharmaceutical company. ÁF and IB have received honoraria for presentation from Chiesi Hungary Ltd. AH is full time employee of Chiesi Hungary Ltd. DL, TC, AT & FM are full time employee of Chiesi Ltd. AEH and JPR are full time employees of the University of Bristol and have received research funding from Chiesi Ltd.

Acknowledgement

Part of this article is based upon work from COST Action MP1404 SimInhale 'Simulation and pharmaceutical technologies for advanced patient-tailored inhaled medicines', supported by COST (European Cooperation in Science and Technology) www.cost.eu.

Appendix A. Supplementary data

Supplementary data associated with this article can be found, in the online version, at http://dx.doi.org/10.1016/j.ijpharm.2017.09.057.

References

Buttini, F., Brambilla, G., Copelli, D., Sisti, V., Balducci, A.G., Bettini, R., Pasquali, I., 2016. Effect of flow rate on in vitro aerodynamic performance of NEXThaler® in comparison with Diskus® and Turbohaler® dry powder inhalers. J. Aerosol Med. Pulm. D. 29, 167–178.

Casaro, D., Brambilla, G., Pasquali, I., 2014. In vitro aerosol performances of NEXThaler® using representative inhalation profiles from asthmatic patients. Respir. Drug Delivery 2, 375–379.

Chan, A.H., Harrison, J., Black, P.N., Mitchell, E.A., Foster, J.M., 2015. Using electronic monitoring devices to measure inhaler adherence: a practical guide for clinicians. J. Allergy Clin. Immun. 3, 335–349.

Cheng, Y.S., Zhou, Y., Su, W., 2015. Deposition of particles in human mouth-throat replicas and a USP induction port. J. Aerosol Med. Pulm. D. 28, 147–155.

Cheng, Y.S., 2003. Aerosol deposition in extrathoracic region. Aerosol Sci. Technol. 37, 659–671.

Corradi, M., Chrystyn, H., Cosio, B.G., Pirozynski, M., Loukides, S., Louis, R., Spinola, M., Usmani, O.S., 2014. NEXThaler, an innovative dry powder inhaler delivering an extrafine fixed combination of beclamethasone and formoterol to treat large and small airways in asthma. Expert Opin. Drug Del. 11, 1497–1506.

Crisafulli, E., Zanini, A., Pisi, G., Pignatti, P., Poli, G., Scuri, M., Chetta, A., 2016. Inhaled beclometasone dipropionate/formoterol fumarate extrafine fixed combination for the treatment of asthma. Expert Rev. Resp. Med. 10, 481–490.

Davies, J.F., Haddrell, A.E., Rickards, A.M.J., Reid, J.P., 2013. Simultaneous analysis of the equilibrium hygroscopicity and water transport kinetics of liquid aerosol. Anal. Chem. 85, 5819–5826.

De Boer, A.H., Gjaltema, D., Hagedoorn, P., Frijlink, H.W., 2015. Can 'extrafine' dry powder aerosols improve aerosol deposition? Eur J. Pharm. Biopharm. 96, 143–151.

Farkas, Á., Jókay, Á., Balásházy, I., Füri, P., Müller, V., Tomisa, G., Horváth, A., 2016. Numerical simulation of emitted particle characteristics and airway deposition distribution of Symbicort® Turbuhaler® dry powder fixed combination aerosol drug. Eur. J. Pharm. Sci. 93, 371–379.

Haddrell, A.E., Davies, J.F., Miles, R.E.H., Reid, J.P., Dailey, L.A., Murnane, D., 2014. Dynamics of aerosol size during inhalation: hygroscopic growth of commercial nebulizer formulations. Int. J. Pharm. 463, 50–61.

Haefeli-Bleuer, B., Weibel, E.R., 1988. Morphometry of the human pulmonary acinus. Anat. Rec. 220, 401–414.

Horváth, A., Balásházy, I., Tomisa, G., Farkas, Á., 2017. Significance of breath-hold time in the dry powder aerosol drug therapy. Eur. J. Pharm. Sci. 104, 145–149.

Jókay, Á., Farkas, Á., Füri, P., Horváth, A., Tomisa, G., Balásházy, I., 2016. Computer modelling of airway deposition distribution of Foster® NEXThaler® and Seretide® Diskus® dry powder combination drugs. Eur. J. Pharm. Sci. 88, 210–218.

Koblinger, L., Hofmann, W., 1990. Monte Carlo Modelling of Aerosol deposition in human lungs: part 1. Simulation of particle transport in a stochastic lung structure. J. Aerosol Sci. 21, 661–674.

Kulmala, M., Vesala, T., Wagner, P.E., 1993. An analytical expression for the rate of binary condensational particle growth. P. Roy. Soc. Lond A. Mat. 441, 589–605.

Mariotti, F., Sergio, F., Acerbi, D., Meyer, T., Herpich, C., 2011. Lung deposition of extrafine dry powder fixed combination beclomethasone dipropionate plus formoterol fumarate via the NEXT DPI® in helathy subjects, asthmatic and COPD patients. Eur. Respir J. 38, 830.

Marple, V.A., Olson, B.A., Santanakrishnan, K., Mitchell, J.P., Muray, S.C., Hudson-Curtis, B.L., 2003. Next generation impactor (A new impactor for pharmaceutical inhaler testing) part II: archival calibration. J. Aerosol Med. 16, 301–324.

Mason, F., Tweedie, A., Lewis, D., 2015. Effect of the Breath-Actuated Mechanism on the dispersion performance of the NEXThaler®. Drug Delivery Lungs 26, 265–269.

Pasquali, I., Merusi, C., Brambilla, G., Long, E.J., Hargrave, G.K., Versteeg, H.K., 2015. Optical diagnostic study of air flow and powder fluidisation in NEXThaler®: Part I: studies with lactose placebo formulation. Int. J. Pharm. 496, 780–791.

Petters, M.D., Kreidenweis, S.M., 2007. A single parameter representation of hygroscopic growth and cloud condensation nucleus activity. Atm. Chem. Phys. 7, 1961–1971.

Raabe, O.G., Yeh, H.C., Schum, G.M., Phalen, R.F., 1976. Tracheobronchial Geometry: Human, Dog, Rat and Hamster. Lovelace Foundation Report (LF-53 Available at). http://mae.engr.ucdavis.edu/wexler/lungs/LF53-Raabe/.

Roberts, D.L., Romay, F.A., Marple, V.A., Miller, N.C., 2000. A high-capacity pre-separator for cascade impactors. Respir. Drug Delivery 7, 443–445.

Rovelli, G., Miles, R.E.H., Reid, J.P., Clegg, S.L., 2016. Accurate measurements of aerosol hygroscopic growth over a wide range in relative humidity. J. Phys. Chem. A. 120, 4376–4388.

Scichilone, N., Spatafora, M., Battaglia, S., Arrigo, R., Benfante, A., Bellia, V., 2013. Lung penetration and patient adherence considerations in the management of asthma: role of extra-fine formulations. J. Asthma Allergy 6, 11–21.

Scuri, M., Alfieri, V., Giorgia, A., Pisi, R., Ferrari, F., Taverna, M., Vezzoli, S., Chetta, A., 2013. Measurement of the inhalation profile through a novel dry powder inhaler (Nexthaler®) in asthmatic patients using acoustic monitoring. Am. J. Resp. Crit. Care 187, A1931.

Tweedie, A., Lewis, D., 2016. Enhancing the performance of dry powder inhalers: breath-actuated mechanisms. ONdrugDelivery 66, 34–38.

Tweedie, A., Mason, F., Lewis, D., 2015. Investigating the effect of modified Breath actuated mechanisms on the dispersion performance of the NEXThaler®. Drug Delivery Lungs 26, 260–264.

Zanker, D., Ehlich, H., Sommerer, K., Mariotti, F., Riolo, D., Cocconi, D., Lutero, E., 2011. Development of a robust technique of radiolabelling beclometasone dipropionate (BDP) with 99mTechnetium in a BDP/Formoterol dry powder inhaler. poster, drug delivery to the lungs. In: DDL Conferences. Edinburgh.

Zhou, Y., Sun, J., Cheng, Y.S., 2011. Comparison of deposition in the USP and physical mouth-throat models with solid and liquid particles. J. Aerosol Med. Pulm. D. 24, 277–284.